

cess offset makes it possible to improve the breakdown voltage to the disadvantage of the drain-source current and microwave capabilities. Hence, a compromise must be found. This model constitutes a reliable simulation tool which appears to be very interesting for the power transistor optimization because it needs a short computing time.

ACKNOWLEDGMENTS

The authors would like to thank the Thomson TCS foundry for making the devices. This work was supported by the DRET (Contract 94160).

REFERENCES

1. J. P. Teysier, J. P. Viaud, and R. Quéré, "A New Nonlinear I(V) Model for FET Devices Including Breakdown Effects," *IEEE Microwave Guided Wave Lett.*, Vol. 4, 1994, pp. 104–106.
2. P. Ellrodt, W. Brockerhoff, and F. J. Tegude, "Simulation of Gate Leakage due to Impact Ionisation in InAlAs/InGaAs-HFET," *4th Int. Seminar on Simulation of Devices and Tech.*, Berg-en-Dal, Nov. 1995, pp. 34–37.
3. C. Gaquière, B. Bonte, D. Théron, Y. Crosnier, P. Arsène-Henri, and T. Pacou, "Breakdown Analysis of an Asymmetrical Double Recessed Power MESFET's," *IEEE Trans. Electron Devices*, Vol. 42, Feb. 1995, pp. 209–214.
4. Y. Butel, J. Hédoire, J. C. De Jaeger, M. Lefebvre, and G. Salmer, "HFET Breakdown Study by 2D and Quasi 2D Simulations: Topology Influence," *Simulation of Semiconductor Devices and Proc.*, Vol. 6, Sept. 1995, pp. 360–363.
5. C. Morton, C. Snowden, and M. Howes "A New Quasi-Two-Dimensional HEMT Model," *Simulation of Semiconductor Devices and Proc.*, Vol. 6, Sept. 1995, pp. 352–355.
6. T. Shawki, G. Salmer, and O. El-Sayed, "MODFET 2D Hydrodynamic Energy Modeling: Optimization of Subquarter-Micron Gate," *IEEE Trans. Electron Devices*, Vol. 31, Jan. 1990, pp. 21–30.
7. J. Dickman, S. Schildberg, A. Geyer, B. E. Maile, A. Schurr, S. Heuthe, and P. Narozny, "Breakdown Mechanisms in the On-State Mode of Operation of InAlAs/In_xGa_{1-x}As Pseudomorphic HEMTs," *6th InP and Related Mater. Conf.*, Santa Barbara, CA, Apr. 1994, pp. 335–338.
8. B. Carnez, A. Cappy, A. Kaszynski, E. Constant, and G. Salmer, "Modelling of a Submicrometer Gate Field-Effect Transistor Including Effects of Non Stationary Electron Dynamics," *J. Appl. Phys.*, Vol. 51, Jan. 1980, pp. 784–790.
9. H. Happy, G. Dambrine, J. Alamkan, F. Danneville, F. Kaptche-Tagne, and A. Cappy, "Helena: A Friendly Software for Calculating the D.C., A.C. and Noise Performance of HEMTs," *Int. J. Microwave Millimeter Wave Computer Aided Eng.*, Vol. 3, No. 1, 1993, pp. 14–28.
10. J. F. Stern, "Self-Consistent Results for n-Type Si Inversion Layers," *Phys. Rev. B*, Vol. 5, No. 12, 1972, pp. 4891–4899.
11. C. Jacoboni and L. Reggiani, "The Monte Carlo Method for the Solution of Charge Transport in Semiconductors with Applications to Covalent Materials," *Rev. Mod. Phys.*, Vol. 55, July 1983, pp. 645–705.
12. Y. Okuto and C. R. Crowell, "Energy Conservation Considerations in the Characterisation of Impact Ionisation in Semiconductors," *Phys. Rev. B*, Vol. 6, No. 8, 1972, pp. 3076–3081.
13. G. A. Baraff, "Distribution Junction and Ionisation Rate for Hot Electrons in Semiconductors," *Phys. Rev.*, No. 128, 1962, p. 2507.
14. C. R. Crowell and S. M. Sze, "Temperature Dependence of Avalanche Multiplication in Semiconductors," *Appl. Phys. Lett.*, No. 9, 1966, p. 242.

ASYMMETRIC FEEDING ACTIVE LEAKY-WAVE ANTENNA ARRAYS

Chien Jen Wang,¹ Jin Jei Wu,² Cheng Chi Hu,¹
and Christina F. Jou¹

¹ Institute of Communication Engineering
National Chiao Tung University
Hsinchu, Taiwan, R.O.C.

² Department of Electric Engineering
Kao Yuan College of Technology and Commerce
Luchu, Kaohsiung, Taiwan, R.O.C.

Received 19 November 1997

ABSTRACT: *The active leaky-wave antenna arrays have been demonstrated, which integrate several microstrip leaky-wave antenna elements with a single HEMT oscillator as an active source at 10.2 GHz. To excite the first higher order mode, the leaky-wave antenna is fed asymmetrically. The reflected wave due to the open end of each leaky-wave antenna element has been suppressed by the symmetric configuration of this antenna array. When comparing with the measured radiation pattern of the single-element antenna, we found that 1×2 and 1×4 antenna arrays can effectively suppress the reflected power by more than 5.5 and 10.5 dB, respectively. Furthermore, the power gains are more than 2 and 3.16 dB higher than the single-element antenna with a measured EIRP of 18.67 dBm. © 1998 John Wiley & Sons, Inc. Microwave Opt Technol Lett 18: 14–17, 1998.*

Key words: *reflected wave; space wave; leaky-wave antenna arrays*

INTRODUCTION

Recently, the leaky-wave antenna has become popular, and there is a growing interest in active-integrated leaky-wave antennas used as frequency-scanning elements [1, 2]. Menzel first discovered the phenomenon of a wider bandwidth in the microstrip leaky-wave antenna compared with resonator antennas [3]. The leaky-wave theory has been derived thoroughly by Oliner [4]. Although the leaky-wave antenna has excellent beam-scanning performance, the reflected wave resulting from the mismatch of the open end of the microstrip antenna may cause the receiving system to mistakenly take the reflected signal for the true signal. For example, the short length ($2.23 \lambda_0$) of Menzel's antenna caused a large back lobe, whose amplitude was about 0.4 of that of the main beam, at the same angle from broadside [4]. The back lobe is produced by the substantial reflected wave caused by the mismatch at the open end. Although it could be improved by using longer strip lines or substrate material of larger height, here, we demonstrate another alternative approach which, using the symmetric configuration of this antenna array, not only can effectively reduce the reflected wave, but also can increase the power gain.

DESIGN

In our experiment, three configurations of the leaky-wave antennas, the 1×1 , 1×2 , and 1×4 arrays, were fabricated. The basic 1×1 configuration shown in Figure 1 consists of an HEMT oscillator as the active source, the matching circuit, and the microstrip leaky-wave antenna. The advantage of one active source, the HEMT oscillator, is that the modes of the arrays do not need to be synchronized. The circuits use 0.635 mm thick RT/duriod substrate with dielectric constant of $\epsilon_r = 10.2$, and NE42484A low-noise GaAs HEMT as the oscillator device. The oscillator is designed using the negative-resistance method utilizing a commercially available CAD

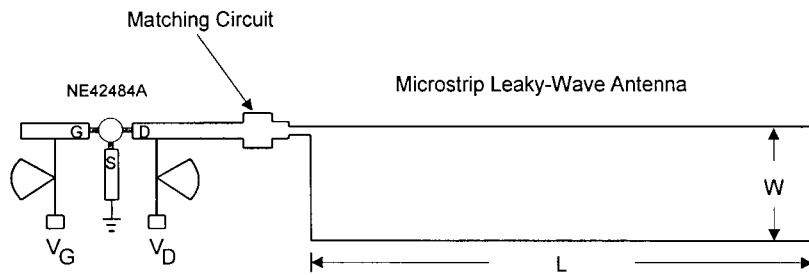


Figure 1 Basic configuration of the hybrid leaky-wave antenna with a low-noise GaAs HEMT NE42484A

tool HP-EEsof Libra. Drain bias is supplied through a typical bias network consisting of a high-impedance $\lambda/4$ line, followed by a quarter-wavelength impedance radial stub, and V_{DS} is set at 2 V. The matching circuit using the impedance-matching method [5] was developed, and we found that the quarter-wave transformer was the most suitable.

The geometry and coordinate system for the microstrip leaky-wave antenna are shown in Figure 2. Each slot will radiate the same field as the magnetic dipole [6, 7], with the equivalent magnetic current density M_S and the equivalent reflected magnetic current density M_{RS} due to the mismatch of the load at the end of the leaky-wave antenna. The ratio of M_{RS}/M_S is a reflected ratio of less than 1. After some calculation [8], the approximate reflected ratio of the reflected wave can be obtained. In our design, to excite the first higher order mode, the microstrip leaky-wave antenna is fed asymmetrically. The width L and length W of the leaky-wave antenna are 4.2 mm and 6.734 cm respectively. The dimension is chosen empirically so that the space wave dominates the radiating power, and the first higher order mode is excited. We employed a rigorous (Wiener-Hopf) solution mentioned by [9] to obtain the normalized complex propagation constant $\beta - j\alpha$ of the first higher order mode in its leak range for the leaky-wave antenna, where β is the phase constant and α is the attenuation constant. The variation of β and α as a function of frequency is shown in Figure 3. Because the operating frequency, 10.2 GHz, is below the cutoff frequency of 10.35 GHz, the normalized phase constant β/k_0 is less than 1, and the space wave dominates the leakage.

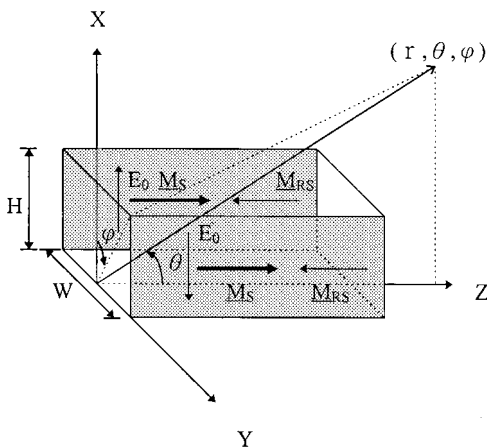


Figure 2 Geometry and coordinate system for the microstrip leaky-wave antenna. M_S is the equivalent magnetic current, and M_{RS} is the equivalent reflected magnetic current

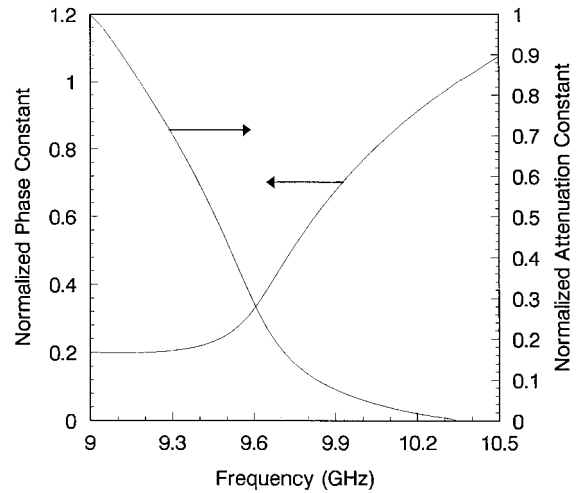


Figure 3 Normalized phase constant β/k_0 and normalized attenuation constant α/k_0 of the first higher order mode as functions of frequency for the leaky-wave antenna. $H = 0.635$ mm, $W = 4.191$ mm, and $\epsilon_r = 10.2$

Figures 4 and 5 show the 1×2 and 1×4 active leaky-wave antenna arrays. We used the impedance-matching theory to design the interelement separation D in order to obtain the minimum reflected coefficient, and D was equal to $0.7 \lambda_0$ (where λ_0 is the free-space wavelength at 10.2 GHz). The simple T -type power divider provides the wide bandwidth. The matching circuit is designed to obtain the maximum radiating power. By this design procedure, the radiator can have maximum power input, and the portion of the reflected wave also can be reduced. In addition, the loading effect will not affect the oscillator's operation.

EXPERIMENTAL RESULTS

Under the far-field condition, Figure 6 shows a comparison of the theoretical and measured H -plane far-field pattern of a single active leaky-wave antenna with the operating frequency at 10.2 GHz. The effective isotropic radiated power (EIRP) of this one-unit antenna is approximately 18.67 dBm. We can see from Figure 6 that the reflected wave (at about an angle of 150°), which is only 3 dB below the main beam, can have an apparently harmful influence on the receiving beam pattern. It is necessary for antenna designers to suppress this reflected wave. Using the configuration of the two-unit and four-unit symmetric antenna arrays (Figs. 4 and 5), we found that the reflected wave of the measured data is effectively suppressed (see Fig. 7). The suppression of the reflected wave for the two-unit and four-unit arrays is about

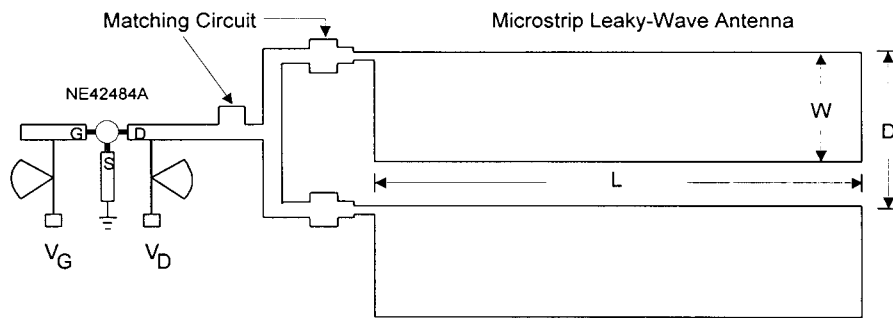


Figure 4 Configuration of the two-unit active leaky-wave antenna array. $D = 0.7 \lambda_0$

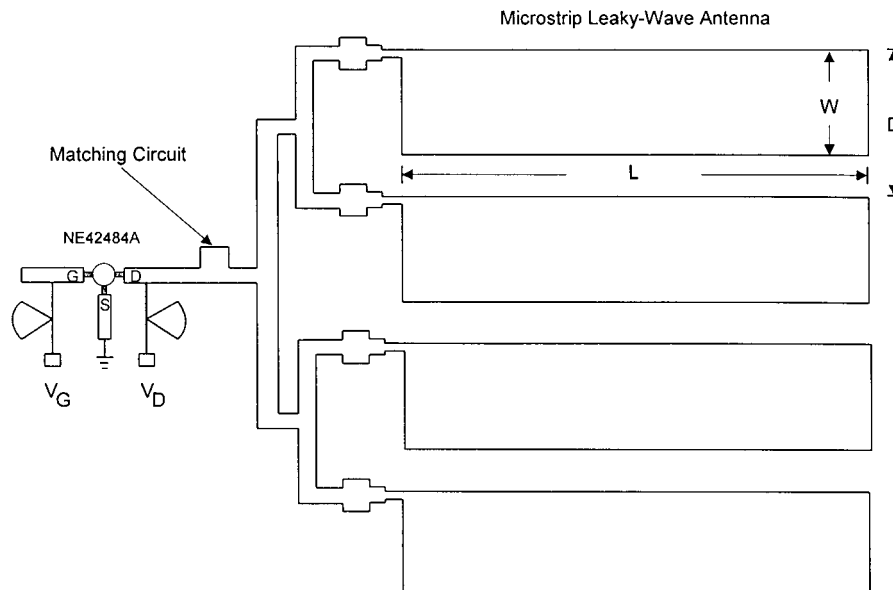


Figure 5 Configuration of the four-unit active leaky-wave antenna array

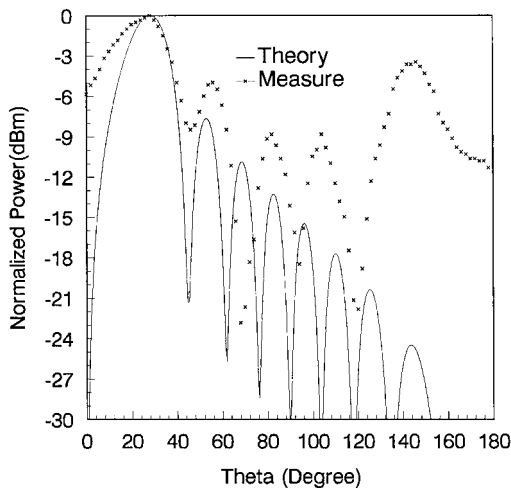


Figure 6 Theoretical and experimental H -plane far-field pattern of single active leaky-wave antenna for the operating frequency at 10.2 GHz

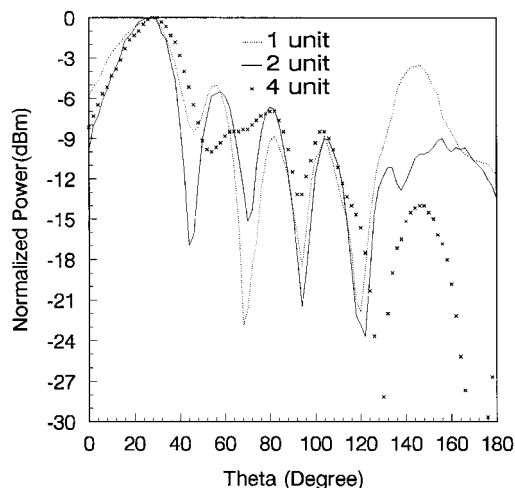


Figure 7 Experimental H -plane far-field patterns of the 1×1 , 1×2 , and 1×4 active leaky-wave antennas, including the arrays

5.5 and 10.5 dB, respectively, when compared with the measured radiation pattern of the single-element antenna. The measured power (EIRP) of the 1×2 and 1×4 symmetric antenna arrays is 20.67 and 21.83 dBm, and the power gains are 2 and 3.16 dB higher than the single-element leaky-wave antenna.

CONCLUSION

The active integrated leaky-wave antenna arrays have been demonstrated in this paper. The advantage of one active source, the HEMT oscillator, is that the arrays do not need to be synchronized. It is found that as the number of elements increases in the symmetric configuration of this an-

tenna array, it not only can have more power gain, but also effectively suppress the reflected signal without using longer lines or substrate material of larger height. Hence, the system can distinguish the true main beam correctly.

ACKNOWLEDGMENT

This work was supported by the National Science Council under Grants NSC 86-2215-E009-31.

REFERENCES

1. A. A. Oliner, "A New Class of Scannable Millimeter Wave Antennas," *Proc. 20th European Microwave Conf.*, 1990, pp. 95–104.
2. C. C. Hu, J. J. Wu, and C. F. Jou, "An Active Frequency-Tuned Beam Scanning Leaky-Wave Antenna," *Microwave Opt. Technol. Lett.*, Jan. 1998.
3. W. Menzel, "A New Traveling Wave Antenna," *Proc. 8th European Microwave Conf.*, 1978, 302–306.
4. A. A. Oliner, "Leakage from Higher Modes on Microstrip with Application to Antennas," *Radio Sci.*, Vol. 22, Nov. 1987, pp. 907–912.
5. D. Pozar, *Microwave Engineering*, Addison-Wesley, Reading, MA, 1990.
6. G. J. Jou and C. K. Tzuang, "Oscillator-Type Active-Integrated Antenna: The Leaky-Mode Approach," *IEEE Trans. Microwave Theory Tech.*, Vol. 44, Dec. 1996, pp. 2265–2272.
7. C. A. Balanis, *Antenna Theory Analysis and Design*, 2nd ed., John Wiley & Sons, New York, 1997.
8. K. S. Lee, "Microstrip Line Leaky Wave Antenna," Ph.D. dissertation, Polytechnic Institute of Brooklyn, NY, 1986.
9. D. C. Chang and E. F. Kuester, "Total and Partial Reflection from the End of a Parallel-Plate Waveguide with an Extended Dielectric Loading," *Radio Sci.*, Vol. 16, Jan.–Feb. 1981, pp. 1–13.

© 1998 John Wiley & Sons, Inc.
CCC 0895-2477/98

A GENERALIZED COMPACT 2-D FDTD MODEL FOR THE ANALYSIS OF GUIDED MODES OF ANISOTROPIC WAVEGUIDES WITH ARBITRARY TENSOR PERMITTIVITY

An Ping Zhao,¹ Jaakko Juntunen² and Antti V. Räsänen²

¹ Electronics Laboratory
Nokia Research Center
FIN-00045 Nokia Group, Finland

² Radio Laboratory
Department of Electrical and Communications Engineering
Helsinki University of Technology
FIN-02150 Espoo, Finland

Received 14 October 1997; revised 19 November 1997

ABSTRACT: In this paper, a generalized 2-D FDTD model based on the \mathbf{D} , \mathbf{E} , and \mathbf{H} fields for the analysis of guided modes of anisotropic waveguides with arbitrary tensor permittivity is proposed. With the help of the proposed model, the relationship between the compact complex and real variable 2-D FDTD methods is investigated. It is found that for certain anisotropic cases, the complex 2-D FDTD method cannot be reduced to (or replaced by) the real variable 2-D FDTD method. On the other hand, excitation techniques for both the complex and real variable methods are also discussed. Numerical results show that using the impulse with complex amplitudes in the excitation is not an essential condition, even for a purely complex 2-D FDTD case. The accuracy and flexibility of the proposed model are validated and confirmed by compar-

ing numerical results with other techniques. © 1998 John Wiley & Sons, Inc. *Microwave Opt Technol Lett* 18: 17–23, 1998.

Key words: compact 2-D FDTD method; guided modes; anisotropic waveguides

1. INTRODUCTION

For numerical modeling of waveguiding structures involving arbitrary geometry and anisotropy, the full-wave analysis technique based on the compact 2-D finite-difference time-domain (FDTD) method has become more and more popular due to its high flexibility. So far, the compact 2-D FDTD technique has been widely employed for the analysis of guided modes of waveguides by many researchers [1–10]. Reviewing the development history of the 2-D FDTD technique, an original 2-D FDTD approach based on a nontruly 2-D mesh was developed [1]. In parallel, a compact 2-D FDTD method, which uses a truly 2-D mesh, and therefore significantly improves the efficiency of the nontruly approach, was proposed [2], and its stability was further investigated [3]. Due to the attractive feature of the compact 2-D FDTD technique [2, 3], nowadays it is being used more than the original 2-D FDTD method [1]. However, the compact 2-D FDTD approaches proposed in [2, 3] were based on the processing of the complex variable, and such a processing was claimed [4] as the disadvantage of the method. In order to overcome this drawback and further improve the efficiency of the compact complex 2-D FDTD method, several real variable algorithms (which are mainly for isotropic and/or diagonal anisotropic cases) based on the 2-D FDTD [4, 6] were developed. The advantage of the real variable method over the complex variable method is obvious since only half of the computer memory and CPU time are required in the real variable algorithm. However, although it was stated in [4] that the real variable 2-D FDTD technique can be applied to arbitrary anisotropic cases, we find that this is not always true. Therefore, it is quite necessary to have a full investigation of the relationship between the complex and real variable methods, and to find out under what conditions the complex variable algorithm can (or cannot) be replaced by the real variable one.

To be able to investigate the above problems, in this paper, a generalized compact 2-D FDTD model based on the \mathbf{D} , \mathbf{E} , and \mathbf{H} fields for the analysis of arbitrary anisotropic dielectric waveguides is developed. With the help of this model, the relationship between the complex 2-D FDTD method and the real variable 2-D FDTD method is comprehensively investigated. Theoretical analysis and numerical results show that when the tangential field components (E_x and/or E_y) are coupled with the longitudinal field component (E_z), the complex 2-D FDTD method cannot be replaced by (or reduced to) the real variable 2-D FDTD method. This means that for some anisotropic cases, the complex 2-D FDTD method has to be employed; and in this paper, such a complex 2-D FDTD method is regarded as the purely complex 2-D FDTD method.

On the other hand, the excitation technique for both the complex and real variable 2-D FDTD methods is also discussed. Even though it was claimed in [1–4, 8] that for the complex 2-D FDTD algorithm the impulse with a (self-evident) complex amplitude must be used in the excitation, it is shown in this paper that using the impulse with complex amplitudes as the excitation is not an essential condition, even for the purely complex 2-D FDTD method. In other